Energy Efficiency of Multiple Antenna Cellular Networks Considering a Realistic Power Consumption Model

Roberto Krauss, Glauber Brante *Member, IEEE,* Ohara Kerusauskas Rayel *Member, IEEE,* Richard Demo Souza *Senior Member, IEEE,* Oluwakayode Onireti *Member, IEEE,* and Muhammad Ali Imran *Senior Member, IEEE*

***Abstract*—We analyze the area energy efficiency (AEE) of a cellular network employing spatial multiplexing (SM), maximal ratio transmission (MRT) and transmit antenna selection (TAS) schemes. Moreover, we consider a realistic power consumption model for small base stations (BSs), which includes the power consumed by the backhaul as well as different interference attenuation levels. Our goal is to maximize the AEE by deploying the optimal number of BSs given some requirements, such as demanded network capacity, amount of interference and employed MIMO scheme. Results show that TAS performs better in terms of AEE when the interference is not fully canceled and for no interference cancellation when the demand for system capacity is lower, while SM becomes more energy efficient when the demanded capacity is higher. Additionally, when the capacity demand and the area to be covered are fixed, we show that although achieving the highest AEE, TAS also demands more small BSs than SM. The system performance in terms of AEE is shown to be strongly dependent on the amount of interference, which in turn depends on the employed interference-mitigation scheme and on the power consumption model.**

***Index Terms*—Area energy efficiency, multiple antennas schemes, power consumption model, small base stations.**

I. Introduction

By 2023, the aggregate mobile traffic is expected to be between 7 and 8 times greater than today [1], [2], resulting in an increase at a compound annual growth rate (CAGR) of about 42%. Around 3.5 connected devices per capita are expected, of which 20 billion will be related to the Internet of Things (IoT) [1], [2]. Such growing demand requires the deployment of more base stations (BSs), which in turn may significantly increase the network power consumption. Since the natural resources used for energy generation are limited and in many cases, non-renewable, there is a global concern about energy efficiency [3]. So, while developing the network plan, maximizing the energy efficiency is the main target. A higher energy efficiency can be achieved by finding the optimal number of BSs to deliver a desired quality of service. Looking forward to improving spectral efficiency, the long-term evolution (LTE) cellular network 4G standard [4] employs multiple antenna (MIMO) technologies aiming to mitigate the effects of fading at the wireless channel, by providing diversity gains through maximum ratio transmission (MRT) techniques, or to increase the network capacity, by providing multiplexing gains through spatial multiplexing (SM) schemes. However, these techniques also lead to a greater energy consumption as a result of the multiple radio frequency (RF) chains, specially due to the power amplifier consumption that corresponds to 55-60% of the total consumption in a BS [3]. By choosing a proper MIMO technique, it has been shown that different goals can be achieved, *e.g.*, meeting the increased traffic demand, or reducing the power consumption [5].

In scenarios where the demanded traffic is not critical, a deployment focused on energy efficiency can rely on the transmit antenna selection (TAS) technique, in which only one RF chain remains active at the transmitter [6]. It is worth noting that LTE already employs TAS, but at the user equipment (UE) only [7], since LTE was first designed to increase the throughput only, not the energy efficiency. In such scenarios, if TAS is employed at the BS side, a greater energy efficiency could be achieved, with the same diversity order as in MRT [8], which could also lead to greater area energy efficiency (AEE). Moreover, according to [5], when analyzed through a realistic power consumption (PCM) model, TAS is more energy efficient when compared to SM in the low to medium spectral efficiency region. However, since only one transmit antenna is selected, the transmit power needed to meet a required spectral efficiency increases at a greater rate for TAS when compared to SM, so that in the high spectral efficiency region SM becomes the best choice. For instance, the authors in [9] were one of the first to show the energy efficiency improvements of antenna selection schemes in wireless sensor networks, specially when the circuitry power consumption is properly taken into account. Later, the work in [10] assessed the energy efficiency performance of TAS in large-scale communication systems. Two different cases are considered there: i.) when the circuit power consumption is comparable to or even dominates the transmit power; and ii.) the circuit power can be ignored due to relatively much higher transmit power. Then, their analysis shows an optimal number of antennas to maximize the energy efficiency in the first case, whereas in the second case, the energy efficiency is maximized when all the available antennas are used. Furthermore, [11] investigates the trade-off between energy efficiency and spectral efficiency in large-scale MIMO systems. As their results show, in order to find Pareto optimal solutions, both energy efficiency and

Roberto Krauss, Glauber Brante and Ohara K. Rayel are with the Federal University of Technology-Paraná (UTFPR), Curitiba, Brazil (e-mails: robertomartinez@alunos.utfpr.edu.br, gbrante@utfpr.edu.br, oharakr@utfpr.edu.br).

Richard D. Souza is with the Federal University of Santa Catarina (UFSC), Florianpolis, Brazil (e-mail: richard.demo@ufsc.br).

Oluwakayode Onireti and Muhammad A. Imran are with University of Glasgow, Glasgow, UK (e-mails: oluwakayode.onireti@glasgow.ac.uk, muhammad.imran@glasgow.ac.uk)

This work has been supported by CAPES and CNPq, Brazil, and by EPSRC (GCRF) funds under the grant EP/P028764/1.

spectral efficiency can be maximized with proper transmit power allocation and optimization on the number of employed antennas.

Moreover, a cross layer approach to the energy efficiency has been carried out in [12], which takes physical and link layers into account. Then, by comparing SM and TAS, the authors provide algorithms to optimize the number of active antennas and the transmit power in this context. In addition, [13] studies the mathematical property of the energy efficiency as a function of the number of antennas. The authors prove that the monotonicity of the energy efficiency function is guaranteed if the system signal-to-noise ratio (SNR) is greater than a given threshold. Then, a low complexity algorithm to select the optimal number of antennas is proposed.

Common to the above is that the analyses in [9]–[13] are only performed from a point-to-point communication perspective, which may considerably change in a dense network scenario. Then, the authors in [14] consider the downlink of a cellular network, where the locations of the BSs are modeled by a Poisson point process (PPP). The energy efficiency of the system is obtained for different antenna configurations under various MIMO schemes. Then, expressions for the coverage, throughput, and power consumption are used to formulate the resource allocation problem for each diversity scheme, with the aim of maximizing the network-wide energy efficiency, while satisfying a minimum QoS constraint.

In addition, when analyzing energy efficiency, it was shown that considering a realistic PCM is important and could lead to contrasting results if the model is not adequately selected [5], [15]–[17]. A realistic PCM should not only take the transmit power into account, but also several other components that consume power in a BS, such as the AC-DC main power unit, cooling and DC-DC power supplies, as well as the RF power amplifier chain for communications. Additionally, in [18], [19] it was shown that the power consumed by the backhaul – *i.e.*, the power consumed by the aggregation switches, which is a function of the network traffic – should not be neglected in a complete network energy efficiency evaluation as it may actually be the bottleneck in terms of energy consumption.

For instance, in order to extend coverage in indoor environments or to increase the AEE, a higher number of BSs could be deployed, leading to a denser network. Nevertheless, severe inter-cell interference may arise due to that, and this problem was first addressed in 3GPP LTE standard release 8 [20], where the inter-cell interference coordination (ICIC) was introduced to allocate different frequency resources to the UEs at the cell edge. Since then, the following LTE releases have improved the interference cancellation techniques, with an *enhanced* ICIC scheme being introduced by releases 9 and 10 [20], allocating different subframes between macro and small cells, while release 11 has introduced a coordinated multi-point transmit and reception (CoMP) approach [21], with dynamic coordination for transmission and reception of signals at multiple cells. With CoMP, one or more BSs can serve one user equipment (UE) in order to mitigate interference and to achieve higher throughputs.

However, the use of CoMP relies on some accuracy level in terms of channel state information (CSI). With high CSI accuracy, the scheduling among users and BSs can be optimally designed [22], achieving high diversity gains. Nevertheless, acquiring accurate CSI in a dense scenario is challenging, so that many sub-optimal quantization approaches are commonly employed [23], [24]. As a consequence, since the transmit precoding has the function of suppressing the interference, imperfections in channel estimation may lead to different levels of interference cancellation [22]. In addition, depending on the size of the cluster controlled by the CoMP technique, some residual inter-cell interference may still persist even with perfect CSI [22]. In any case, CSI must be constantly shared between UEs and BSs in order to make scheduling possible, which due to imperfections in channel estimation and the number of served UEs may lead to different levels of interference cancellation.

In this paper, we analyze the energy efficiency of SM, MRT and TAS in the downlink of a cellular network consisting of small BSs, constrained to a minimum received power for the users at the cell edge. In this scenario, the UE is subjected to interference from other neighbor small BSs. We assume that interference may not be fully canceled due to, *e.g.*, the interference mitigation technique or imperfect CSI estimation, so that we consider a fraction of residual interference denoted by κ, which may also reduce the energy and spectral efficiency in dense deployments [25]. Moreover, we employ a realistic PCM that combines [5] and [19], *i.e.*, it scales with the number of active antennas at the BS for the different MIMO techniques [5], at the same time, it includes the backhaul power consumption [19]. Due to the consideration in our analysis that the interference may not be fully canceled, and due to the employment of a realistic PCM, we observe different trade-offs in terms of AEE between the MIMO techniques when compared to the results presented in [15]–[17]. We analyze several scenarios including variations on the demanded capacity, number of antennas, interference level and area to be covered. We show that the AEE can be maximized by a proper selection of the system deployment parameters.

A. *Contributions*

This paper extends our previous preliminary results from [26]. The contributions of this work can be summarized as follows:

- We observe different trade-offs in terms of AEE between the MIMO techniques than those found in [15]–[17]. For instance, TAS stands out with the largest AEE when the demand for system capacity is low and the inter-cell interference is not fully canceled, while SM becomes more energy efficient when the capacity demand is larger or when there is full interference cancellation;
- We also show that the energy efficiency results can be significantly different depending on the employed PCM, *e.g.*, if the backhaul or the fraction that scales with the number of antennas are considered or not, it could lead to an unrealistic performance prediction;
- We observe that, as the number of antennas increases, TAS becomes the most energy efficient scheme, as its AEE only increases with the number of antennas, whilst

SM and MRT have an optimal performance when a 4×4 scheme is considered. Moreover, by fixing the number of BSs and varying the area to be covered, we show that TAS is the most energy efficient scheme for a low interference level.
- We emphasize that when TAS is the most energy efficient scheme, it always needs more BSs to achieve the same area throughput as SM, since its multiplexing gain is smaller. Thus, the trade-off between the capital expenditure (CAPEX) for network deployment and the energy savings need to be taken into account by the stakeholders;
- Finally, the performance in terms of AEE is shown to be strongly dependent on κ, so that conclusions in terms of which MIMO scheme achieves the largest AEE may change with the performance of the interference mitigation technique in use.

B. Organization and Notations

The remainder of this paper is organized as follows. Section II presents the system model, including the network total power and the AEE definition, while Section III depicts the considered MIMO schemes: SM, MRT and TAS. Numerical examples are given in Section IV, while Section V concludes the paper.

In terms of notations, we use bold upper case letters to denote matrices, like $\mathbf{H}$, and bold lower case letters to represent vectors, as $\mathbf{x}$, whose transpose conjugate is denoted by $\mathbf{x}^\dagger$. Scalars are represented by non-bold letters, as x, and their average is denoted by $\overline{x}$. The complete list of symbols used throughout this paper is given by Table I.

TABLE I
LIST OF SYMBOLS

Parameter	Description
N_{BS}	Number of required base stations
P_{L}	Path loss
G	Antenna gain
L	Link margin
λ	Wavelength
α	Path-loss exponent
A	Coverage area
P_{tx}	Transmit power
$\mathbf{H}$	Channel matrix
$h_{i,j}$	Fading coefficients
m_{t}	Number of transmit antennas
$\widehat{m}_{\text{t}}$	Number of active transmit antennas
m_{r}	Number of receive antennas
$\mathbf{x}$	Unit energy transmitted symbol
$\mathbf{y}$	Received symbol
$\mathbf{w}$	Zero-mean Additive White Gaussian Noise
d	Transmission distance
$\overline{\gamma}$	Average signal-to-noise ratio (SNR)
W	Channel bandwidth
κ	Interference cancellation level
ζ	Signal-to-interference ratio (SIR)
P_{I}	Interference power (PI)
Γ	Average signal-to-interference-plus-noise ratio (SINR)
P_{net}	Network total power consumption
P_0	Amplifier, cooling, power supply and battery losses
P_1	Circuitry power consumption that depends on $\widehat{m}_{\text{t}}$
P_2	Circuitry power consumption independent from $\widehat{m}_{\text{t}}$
$\max_{\text{dl}}$	Maximum number of downlink interfaces
P_{bh}	Backhaul power consumption
P_{s}	Power consumed by each access switch
P_{dl}	Power consumed by the downlink interfaces
P_{ul}	Power consumed by the uplink interfaces
N_{ul}	Number of uplink interfaces
Ag_{tot}	Total traffic aggregated at all switches
$U_{\max}$	Maximum rate supported by each uplink interface
Ag_{switch}	Traffic traversing the switch
$Ag_{\max}$	Maximum traffic supported by the switch
δ	Parameter that reflects the weight of Ag_{switch} on P_{s}
$P_{\text{s,max}}$	Maximum power consumed by the switch
Ω	Area power consumption
τ_A	Area throughput targets
η_A	Energy efficiency metric in bits/J/km^2
$C_{\text{net}}^{(\text{SM})}$	Capacity of the Spatial Multiplexing scheme
$\overline{\gamma}_{\text{SM}}$	Average SNR per receive antenna for SM
m	Minimum between m_{t} and m_{r}
$\mathbf{I}_m$	$m\times m$ identity matrix
$\mathbf{\Xi}$	$\mathbf{H}\mathbf{H}^\dagger$ when $m_{\text{t}}\geq m_{\text{r}}$ or $\mathbf{H}^\dagger\mathbf{H}$ when $m_{\text{t}}<m_{\text{r}}$
$\lambda_{\max}$	Maximum eigenvalue of $\mathbf{\Xi}$
$C_{\text{net}}^{(\text{MRT})}$	Capacity of the Maximum Ratio Transmission scheme
γ_{MRT}	Instantaneous SNR at the receiver for MRT
$C_{\text{net}}^{(\text{TAS})}$	Capacity of the Transmit Antenna Selection scheme
γ_{TAS}	Instantaneous SNR at the receiver for TAS
$P_{\min}$	Minimum required power at cell edge
f	Carrier frequency
N_0	Noise psd/Hz
$P_{\max}$	Maximum transmit power for each BS
$U_{\max}$	Maximum rate at each uplink interface

II. PRELIMINARIES

A. System Model

Let us consider a cellular network composed by hexagonal cells of radius R, covering an area of A km^2, as illustrated in Figure 1. Then, the number of required BSs can be written as

$$N_{\text{BS}}=\frac{2A}{3\sqrt{3}R^2}. \tag{1}$$

In the downlink direction, the signal transmitted by the BS and received by the UE is given by [27]

$$\mathbf{y}=\sqrt{\frac{P_{\text{L}}\,P_{\text{tx}}}{\widehat{m}_{\text{t}}}}\,\mathbf{H}\,\mathbf{x}+\mathbf{w}, \tag{2}$$

where P_{tx} is the transmit power of the BS, $\mathbf{H}\in\mathbb{C}^{m_{\text{r}}\times\widehat{m}_{\text{t}}}$ is the channel matrix composed by the fading coefficients $h_{i,j}$, where m_{t} is the number of transmit antennas, $\widehat{m}_{\text{t}}$ is the number of *active* transmit antennas[1], m_{r} is the number of receiving antennas, $\mathbf{x}\in\mathbb{C}^{\widehat{m}_{\text{t}}\times1}$ is the unit energy transmitted symbol vector, $\mathbf{y}\in\mathbb{C}^{m_{\text{r}}\times1}$ is the received symbol vector and $\mathbf{w}\in\mathbb{C}^{m_{\text{r}}\times1}$ is the zero-mean additive white Gaussian noise with variance $N_0/2$ per dimension, where N_0 is the thermal noise power spectral density per Hertz. Also, without loss of generality, we consider $m_{\text{t}}=m_{\text{r}}$ throughout this paper, which we denote by number of antennas.

[1]Notice that $\widehat{m}_{\text{t}}\leq m_{\text{t}}$, while the active antennas are selected according to the employed MIMO transmission scheme.

Moreover, the path-loss is [27]

$$P_{\text{L}}=\frac{G\lambda^2}{L(4\pi)^2d^\alpha}, \tag{3}$$

where α is the path loss exponent in a urban microcells environment, d is the transmission distance, G is the antenna gain, L is the link margin and λ is the wavelength.

Then, the average SNR per receive antenna is

$$\overline{\gamma}=\frac{P_{\text{L}}P_{\text{tx}}}{N_0W}, \tag{4}$$

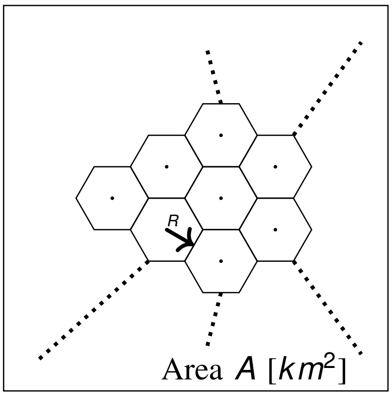

Fig. 1. System model of a cellular network composed by $N_{\rm BS}$ hexagonal cells of radius R, covering an area A.

where W is the channel bandwidth.

Moreover, we also consider that the communication links are subjected to interference, which may not be fully canceled depending on the employed interference mitigation scheme, so that in our model we include a factor denoted by $\kappa \in [0,1]$ that multiplies the maximum interference power $P_{\rm I}$. Thus, the signal-to-interference power ratio (SIR) in the case of hexagonal cells becomes [27]

$$\zeta = \frac{P_{\rm L} P_{\rm tx}}{\kappa P_{\rm I}}, \tag{5}$$

in which $\kappa = 0$ yields $\zeta \to \infty$, *i.e.*, full interference cancellation, while $\kappa = 1$ considers the worst-case scenario with no interference cancellation at all.

The average SINR for the UE at the cell edge is

$$\Gamma = \frac{P_{\rm L} P_{\rm tx}}{N_0 W + \kappa P_{\rm I}} = \frac{\overline{\gamma}}{1+\overline{\gamma}\,\zeta^{-1}}. \tag{6}$$

B. Network Total Power

To compute the network total power consumption, $P_{\rm net}$, we employ a PCM combining [5] and [19], which also takes into account the number of active antennas at the BS. Thus,

$$P_{\rm net} = N_{\rm BS}\left[\widehat{m}_{\rm t}(P_0 P_{\rm tx} + P_1) + P_2)\right] + P_{\rm bh}, \tag{7}$$

where P_0 is a constant that encompasses the effects of the power amplifier drain efficiency, cooling, power supply and battery backup losses, P_1 represents the part of the circuitry power consumption that grows linearly with $\widehat{m}_{\rm t}$, while P_2 is the power consumption that does not depend on $\widehat{m}_{\rm t}$ [5], [15]. Moreover, $P_{\rm bh}$ is the power consumption of the backhaul[2].

Furthermore, as depicted in Figure 2, the power consumed by the backhaul takes into account the power consumed by the downlink interfaces ($P_{\rm dl}$), dedicated to each BS, the uplink interfaces ($P_{\rm ul}$), dedicated to each access switch, and the power consumed by the access switch ($P_{\rm s}$), being written as [19]

$$P_{\rm bh} = \left\lceil \frac{N_{\rm BS}}{\max_{\rm dl}} \right\rceil P_{\rm s} + N_{\rm BS} P_{\rm dl} + N_{\rm ul} P_{\rm ul}, \tag{8}$$

where $\lceil . \rceil$ is the ceil operation, $\max_{\rm dl}$ is the maximum number of downlink interfaces available in an aggregation switch and

[2]Let us remark that $P_{\rm bh} = 0$ in [5], while $P_1 = 0$ in [19].

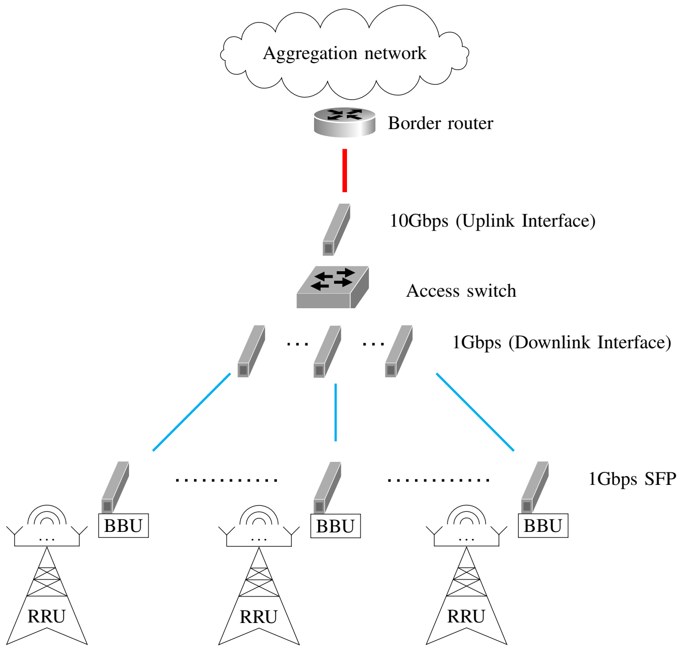

Fig. 2. Backhauling Layout. The Radio Remote Units (RRUs) are connect via wireless channel to the Baseband Units (BBUs). Then, the optical backhaul consists of 1 Gbps SFPs (Small Form-Factor Pluggable) connected to the access switch, by its turn connected through a 10 Gbps interface to the border router.

$N_{\rm ul} = \left\lceil \frac{Ag_{\rm tot}}{U_{\rm max}} \right\rceil$ is the number of uplink interfaces (number of ports used by the switch), where $Ag_{\rm tot}$ is the total traffic aggregated at all switches and $U_{\rm max}$ is the maximum rate supported by each uplink interface.

In addition, the power consumed by each access switch is [19]

$$P_{\rm s} = \delta P_{\rm s,max} + (1-\delta)\frac{Ag_{\rm switch}}{Ag_{\rm max}} P_{\rm s,max}, \tag{9}$$

where $\delta \in [0,1]$ is a weighting parameter, $P_{\rm s,max}$ is the maximum power consumed by the switch, $Ag_{\rm switch}$ is the traffic traversing the switch, and $Ag_{\rm max}$ is the maximum traffic supported by the switch. It is worth noting that the term $Ag_{\rm switch}/Ag_{\rm max}$ in (9) expresses the percentage of traffic transversing the switch, which is related to the number of ports that are occupied.

C. Area Energy Efficiency

In order to compare networks with different cell sizes, we define the area power consumption in W/km^2 as [18]

$$\Omega = \frac{P_{\rm net}}{A}, \tag{10}$$

while we also assume that the cells may have different area throughput targets, which can be written as [19]

$$\tau_A = \frac{C_{\rm net}}{A}, \tag{11}$$

where $C_{\rm net}$ is the total network capacity, which is different depending on the employed MIMO scheme, as will be detailed in Section III. Finally, to reflect the ratio between the overall network capacity and the energy consumption, we adopt an AEE metric, in bits/J/km^2, given by [28]

$$\eta_A = \frac{\tau_A}{P_{\text{net}}}. \tag{12}$$

III. MIMO Transmission Schemes

In this section, we define the SNR and the network capacity for three MIMO schemes, namely spatial multiplexing (SM), maximal ratio transmission (MRT) and transmit antenna selection (TAS). Moreover, let us remark that we restrict our investigation to techniques that are available in current deployments, especially for small BSs, and we leave other approaches such as Massive MIMO [29] for future investigations.

A. Spatial Multiplexing (SM)

In order to exploit the multiplexing gains provided by multiple antennas, SM transmits $m = \min\{m_{\text{t}}, m_{\text{r}}\}$ independent and separate encoded data streams, one by each transmit antenna[3]. Then, the average SNR per receive antenna is [5]

$$\overline{\gamma}_{\text{SM}} = \frac{\overline{\gamma}}{m}, \tag{13}$$

while the capacity of the SM scheme is [5], [30]

$$C_{\text{net}}^{(\text{SM})} = N_{\text{BS}}\ W\ \log_2\left[\det\left(\mathbf{I}_m + \frac{\overline{\gamma}_{\text{SM}}\ \boldsymbol{\Xi}}{1+\overline{\gamma}_{\text{SM}}\ \zeta^{-1}\ \boldsymbol{\Xi}}\right)\right], \tag{14}$$

where $\mathbf{I}_m$ is an $m \times m$ identity matrix and $\boldsymbol{\Xi} \in \mathbb{C}^{m\times m}$ corresponds to a random matrix given by

$$\boldsymbol{\Xi} = \begin{cases} \mathbf{H}\mathbf{H}^{\dagger} & m_{\text{t}} \geq m_{\text{r}} \\ \mathbf{H}^{\dagger}\mathbf{H} & m_{\text{t}} < m_{\text{r}} \end{cases}, \tag{15}$$

with $\mathbf{H}^{\dagger}$ being the conjugate transpose of $\mathbf{H}$.

B. Maximal Ratio Transmission (MRT)

Differently from SM, MRT exploits channel knowledge at the transmitter and at the receiver in order to mitigate the effects of fading [31]. Thus, the same symbol is transmitted over all m_{t} antennas, so that the instantaneous SNR at the receiver is

$$\gamma_{\text{MRT}} = \overline{\gamma}\ \lambda_{\text{max}}, \tag{16}$$

where λ_{max} is the maximum eigenvalue of $\boldsymbol{\Xi}$ in (15).

Then, the capacity for the MRT technique is given by [5], [31]

$$C_{\text{net}}^{(\text{MRT})} = N_{\text{BS}}\ W\ \log_2\left(1 + \frac{\gamma_{\text{MRT}}}{1+\zeta^{-1}\ \gamma_{\text{MRT}}}\right). \tag{17}$$

[3]In the SM and MRT schemes we consider that all transmit antennas are active ($\widehat{m}_{\text{t}} = m_{\text{t}}$).

TABLE II
System Parameters

Parameter	Value
A	40 km^2
G	10 dBi
L	10 dB
α	3.5
P_{min}	-100 dBm
f	2.5 GHz
W	5 MHz
N_0	-174 dBm
P_{max}	6.31 W
P_0	3.14
P_1	35 W
P_2	34 W
U_{max}	10 Gbps
δ	0.9
max_{dl}	24
Ag_{max}	24 Gbps
$P_{\text{s,max}}$	300 W
P_{ul}	2 W
P_{dl}	1 W

C. Transmit Antenna Selection (TAS)

When TAS is employed, we assume that only $\widehat{m}_{\text{t}} = 1$ antenna is selected from the set of m_{t} transmit antennas, which saves power since only one RF chain remains active. Assuming maximum ratio combining (MRC) at the receiver side, the instantaneous SNR of TAS is [27]

$$\gamma_{\text{TAS}} = \overline{\gamma}\ \max_i \sum_{j=1}^{m_{\text{r}}} |h_{i,j}|^2, \tag{18}$$

where the maximum over i represents that only the best antenna of the transmitter is chosen, while the sum comes from the MRC at the receiver.

Thus, the capacity of TAS yields

$$C_{\text{net}}^{(\text{TAS})} = N_{\text{BS}}\ W\ \log_2\left(1 + \frac{\gamma_{\text{TAS}}}{1+\zeta^{-1}\ \gamma_{\text{TAS}}}\right). \tag{19}$$

IV. Numerical results

In this section, a few numerical results are presented. The simulation parameters are shown in Table II, according to [18], with the constants regarding small BS power consumption based on [5], [16] and with the power consumption parameters associated with the backhaul following [19].

A. Area Power Consumption

Let us first analyze the area power consumption (Ω) as a function of the area throughput (τ_{A}). For each scenario, there is a minimum N_{BS} required to cover the area A, which is obtained respecting the maximum transmit power P_{max} for each BS, while guaranteeing a minimum received power P_{min} for the UEs at the cell edge. Moreover, we also consider that a maximum of $N_{\text{BS}} = 500$ can be deployed.

Figure 3 plots Ω as a function of τ_{A} in the case that only small BSs are employed. From the figure, we can notice that TAS minimizes the area power consumption when $\kappa > 0$. Only when there is no interference at the cell edge ($\kappa = 0$), SM performs better than TAS due to the multiplexing gains that provide the required system capacity. However, when κ

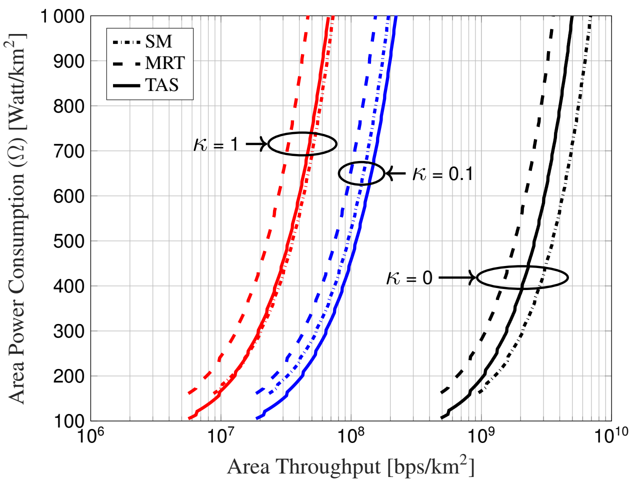

Fig. 3. Area power consumption (Ω) as a function of the area throughput (τ_A), varying N_{BS}, with $m_t = m_r = 2$.

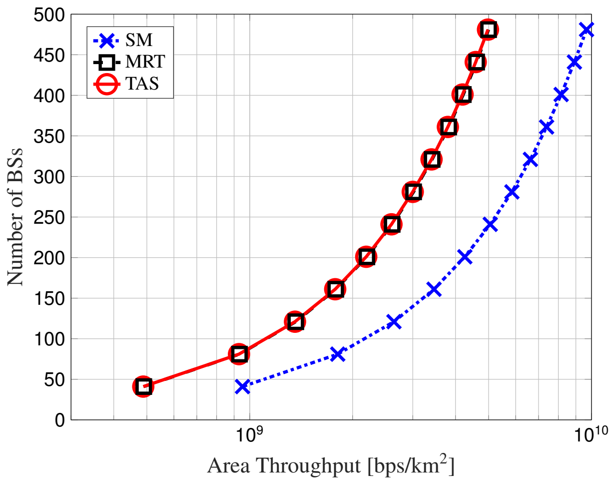

Fig. 4. Number of BSs (N_{BS}) as a function of the area throughput (τ_A), with $m_t = m_r = 2$ and $\kappa = 0$.

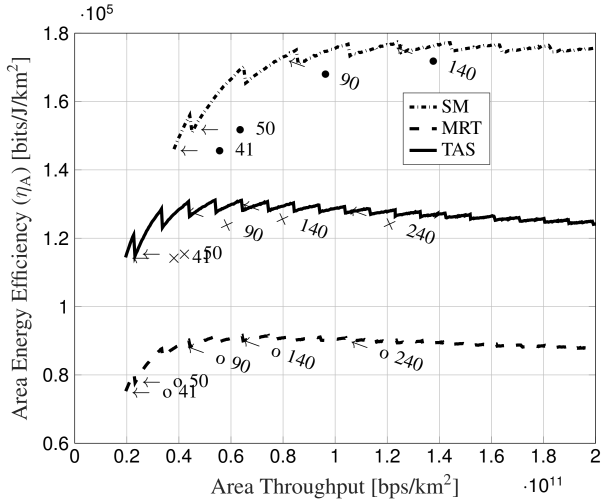

Fig. 5. Area energy efficiency (η_A) as a function of the area throughput (τ_A) for small BSs with $m_t = m_r = 2$ and $\kappa = 0$. The arrow "$\leftarrow \bullet$" indicates the N_{BS} employed by SM, "$\leftarrow \times$" the N_{BS} employed by TAS and "$\leftarrow$ o" the N_{BS} employed by MRT.

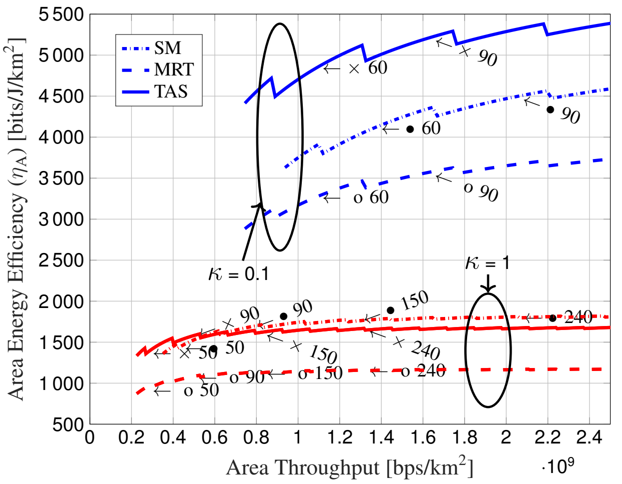

Fig. 6. Area energy efficiency (η_A) as a function of τ_A for small BSs with $m_t = m_r = 2$ and $\kappa = \{0.1, 1\}$.

increases, the higher SNR provided by SM affects both the numerator and denominator of the SINR in (14), so that the smaller number of active RF chains yields the lowest area power consumption for the TAS scheme.

The analysis of Figure 3 is complemented by Figure 4, showing the number of employed BSs (N_{BS}) as a function of τ_A. As we can see, MRT and TAS employ the same N_{BS}, which corroborates with the results in [5] showing that the capacity of the MRT scheme is only slightly larger than that of TAS. Then, the higher area power consumption of MRT with respect to TAS in Figure 3 comes mainly due to the increased power consumption of the antenna RF chains. By its turn, N_{BS} is considerably decreased for the SM scheme due to the multiplexing gains, especially at high τ_A.

Moreover, an interesting behavior caused by the backhaul power consumption is displayed in Figure 3. According to (9), when a new switch must be turned on to support the traffic demand through the backhaul, 90% of $P_{s,max}$ is consumed (due to the term δ in Table II), which is higher than the power consumption of the network (P_{net}) in the case of small BS. Thus, the curves exhibit a slight saw shape, indicating when a new switch starts.

B. Area Energy Efficiency

In this subsection, we analyze the AEE (η_A) as a function of τ_A, with $m_t = m_r = 2$. First, in Figure 5, η_A is evaluated in a scenario where the interference is considered to be fully canceled ($\kappa = 0$). As we can observe, TAS performs better than MRT, while SM has the best performance in this particular scenario. In addition, "$\leftarrow \bullet$" indicates the N_{BS} employed by SM, "$\leftarrow \times$" the N_{BS} employed by TAS and "$\leftarrow$ o" the N_{BS} employed by MRT.

Next, Figure 6 presents the same analysis as in Figure 5, but considering that $\kappa = 0.1$ (interference is not fully canceled) and $\kappa = 1$ (no interference cancellation at all). As we can observe, this analysis corroborates with the results of Figure 3, so that TAS achieves the best performance when $\kappa = 0.1$. In

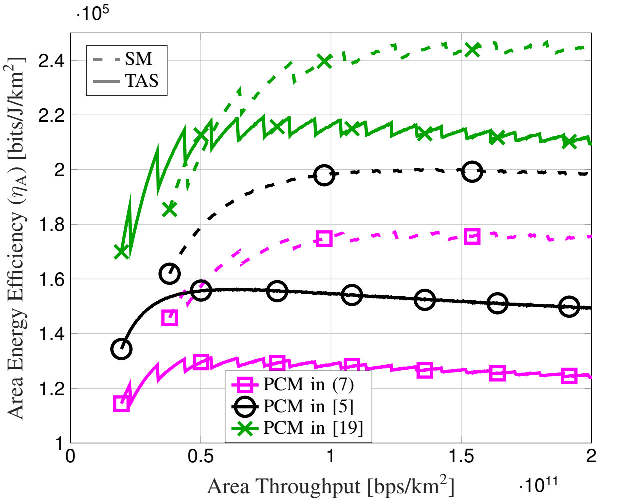

Fig. 7. Area energy efficiency (η_{A}) as a function of the area throughput (τ_{A}) for small BSs with $m_{\mathrm{t}} = m_{\mathrm{r}} = 2$ and $\kappa = 0$. The PCM in [5] considers that $P_{\mathrm{bh}} = 0$, while the PCM in [19] considers $P_1 = 0$.

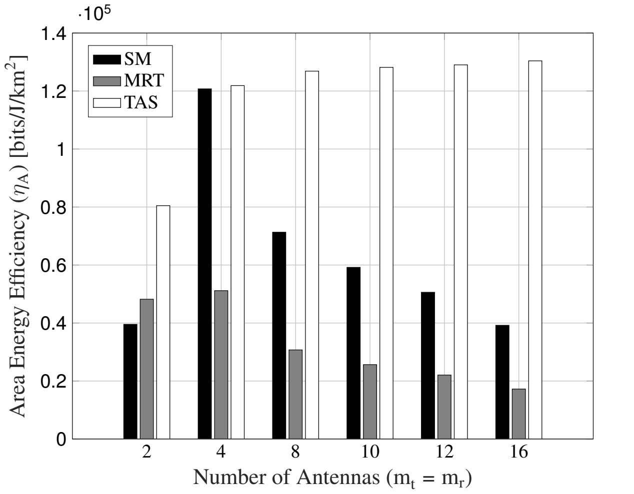

Fig. 8. Area energy efficiency (η_{A}) as a function of the number of antennas ($m_t = m_r$) with $\kappa = 0$, and with a capacity target of 10 Gbits/s and $N_{\mathrm{BS}} = 10$ for SM technique, $N_{\mathrm{BS}} = 21$ for TAS and MRT techniques.

this case, it is interesting to notice that when a fixed N_{BS} is chosen for $\kappa = 0.1$, TAS is more energy efficient than SM and MRT, but SM yields a higher area throughput. Furthermore, the same intersection between TAS and SM is observed when $\kappa = 1$, so that TAS has higher η_{A} when $\tau_{\mathrm{A}} < 526$ Mbps/km^2, while SM performs better when τ_{A} increases. Finally, it is also worth noting from Figures 5 and 6 that even when TAS is more energy efficient than SM, it requires a higher number of deployed BSs.

C. Different Power Consumption Models

The effect of different PCMs is illustrated in Figure 7, where we only compare the AEE of SM and TAS for the sake of a better visualization. In the figure, besides the power consumption model depicted by (7), we also consider the models presented by [5], which does not include the backhaul power consumption (*i.e.*, $P_{\mathrm{bh}} = 0$), and the model in [19], which does not include the fraction of the power that scales with $\widehat{m}_{\mathrm{t}}$ (*i.e.*, $P_1 = 0$).

As we observe, the intersection between TAS and SM changes depending on the considered PCM. For instance, PCM in [19] yields an optimistic assumption for the energy efficiency, once some fraction of power spent by the BSs in idle mode is not considered. Moreover, by comparing the PCMs in (7) and that from [5], we observe that it is crucial to take P_{bh} into account, since it considerably changes the energy efficiency results, which are rather optimistic when $P_{\mathrm{bh}} = 0$.

D. Fixed Network Capacity and Area Energy Efficiency

Figure 8 evaluates η_{A} as a function of the number of antennas ($m_{\mathrm{t}} = m_{\mathrm{r}}$), with $\kappa = 0$ and a target network capacity of $C_{\mathrm{net}} = 10$ Gbits/s. Moreover, the required number of BSs is calculated for the case when $m_{\mathrm{t}} = m_{\mathrm{r}} = 2$, and it remains fixed while we increase the number of antennas. For instance, $N_{\mathrm{BS}} = 10$ is required by the SM technique when $m_{\mathrm{t}} = m_{\mathrm{r}} = 2$, and $N_{\mathrm{BS}} = 21$ is needed for TAS and MRT, which are maintained when we increase $m_{\mathrm{t}} = m_{\mathrm{r}}$ once the goal is to analyze the effect of increasing the number of antennas in an existing network deployment.

As we observe, SM and MRT exhibit a maximal performance when $m_{\mathrm{t}} = m_{\mathrm{r}} = 4$, which is due to the fact that the energy consumption also scales with the number of antennas, limiting the AEE. On the other hand, the AEE using the TAS technique is an increasing function with the number of antennas, although we observe a saturation effect when $m_{\mathrm{t}} = m_{\mathrm{r}} > 10$.

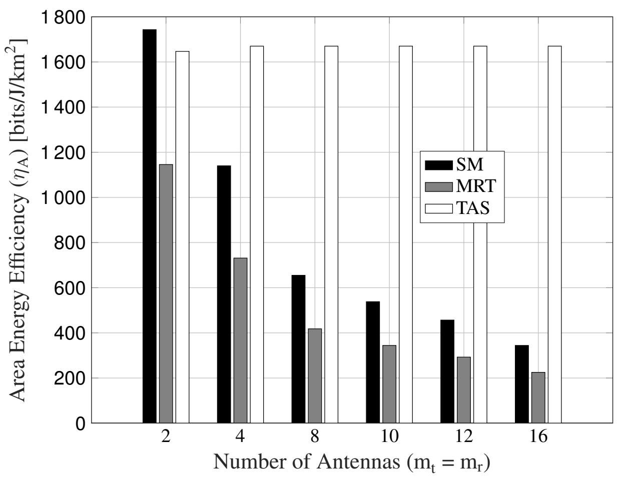

Fig. 9. Area energy efficiency (η_{A}) as a function of the number of antennas ($m_t = m_r$) with $\kappa = 1$, and with a capacity target of 1 Gbits/s and $N_{\mathrm{BS}} = 117$ for SM technique, $N_{\mathrm{BS}} = 183$ for TAS and MRT techniques.

Nevertheless, it is interesting to notice that the performance may change depending on the number of antennas and amount of interference. For instance, Figure 9 plots the AEE as a function of the number of antennas in a scenario without interference cancellation ($\kappa = 1$). As we observe, the performance decreases for SM and MRT when the number of antennas increase, while η_{A} is practically constant for the TAS scheme. Figure 10 complements the analysis by plotting the area power

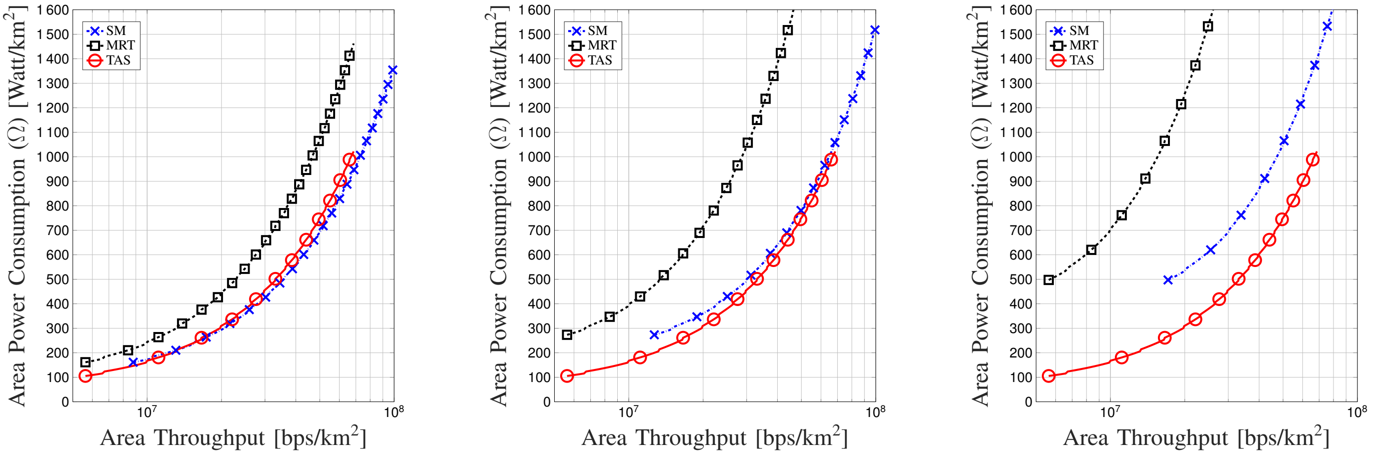

(a) $m_{\mathrm{t}} = m_{\mathrm{r}} = 2$ (b) $m_{\mathrm{t}} = m_{\mathrm{r}} = 4$ (c) $m_{\mathrm{t}} = m_{\mathrm{r}} = 8$

Fig. 10. Area power consumption (Ω) as a function of the area throughput (τ_{A}), for different antenna configurations with $\kappa = 1$.

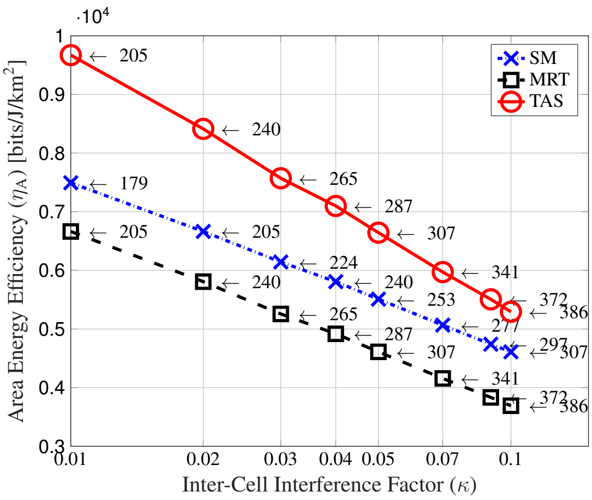

Fig. 11. Area energy efficiency (η_{A}) as a function of κ for $m_t = m_r = 2$, and with a capacity target of 7 Gbits/s.

consumption as a function of the area throughput for $\kappa = 1$ and three different antenna arrangements, with $m_{\mathrm{t}} = m_{\mathrm{r}} = 2$ in Figure 10a, $m_{\mathrm{t}} = m_{\mathrm{r}} = 4$ in Figure 10b, and $m_{\mathrm{t}} = m_{\mathrm{r}} = 8$ in Figure 10c. As the figures show, the performance of TAS slightly increases with the number of antennas, while the power consumption for SM and MRT considerably increases. Nevertheless, we also notice that the area throughput achieved by TAS with $N_{\mathrm{BS}} = 500$ is still much smaller than that of SM with the same antenna configuration.

Furthermore, Figure 11 evaluates the area power consumption as a function of κ, with $m_{\mathrm{t}} = m_{\mathrm{r}} = 2$ and a target network capacity of $C_{\mathrm{net}} = 7$ Gbits/s. Consistent with Figure 8, TAS achieves the highest AEE in this scenario. However, it is interesting to notice that this increased performance comes at the cost of employing more small BSs than SM to supply the same target network capacity.

E. Area Energy Efficiency for Different Coverage Areas

Finally, we evaluate the AEE for different coverage areas, while maintaining N_{BS} fixed. Then, for different coverage areas, we evaluate the AEE in order to ensure that the users at the cell edge obtain $P_{\mathrm{min}} = -100$ dBm, subjected to the transmit power constraint $P_{\mathrm{tx}} \leq P_{\mathrm{max}}$. In this particular scenario, we consider that $N_{\mathrm{BS}} = 80$ and $m_t = m_r = 2$, with $\kappa = 0.1$ in Figure 12 and $\kappa = 1$ in Figure 13.

As Figure 12 shows, TAS outperforms the other schemes in terms of AEE, regardless of the coverage area, which corroborates with the results of Figures 3 and 6. Moreover, as the coverage area increases, the coverage radius of each BS also increases, which demands more transmission power per cell and as a consequence η_{A} decreases with A.

When $\kappa = 1$, Figure 13 shows a slightly better performance of SM compared to TAS and MRT. Interestingly, the performance of SM and TAS in terms of AEE is very similar when $A \geq 40$ km^2, with TAS slightly outperforming SM when $A = 70$ km^2.

V. Final Comments

In this paper, we evaluated a cellular network employing three different multiple antenna techniques: SM, MRT and TAS. The goal is to optimize the AEE by calculating the optimal number of BSs given some requirements, such as demanded network capacity, amount of interference and employed MIMO scheme. Our results show that SM and TAS usually achieve the best performance in terms of area power consumption and AEE. For instance, TAS performs better when the interference is not fully canceled and for no interference cancellation when the demand for system capacity is lower, while SM becomes more energy efficient when the demanded capacity is higher.

Additionally, when the capacity demand and the area to be covered are fixed, we also show that although achieving the highest AEE, TAS also demands more BSs than SM. Finally, the system performance in terms of AEE is shown to be strongly dependent on the amount of interference, which in

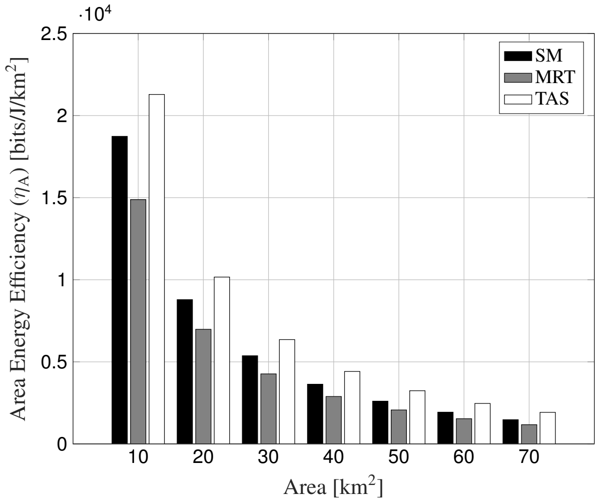

Fig. 12. Area energy efficiency (η_{A}) as a function of the coverage area with $\kappa = 0.1$ and $N_{\mathrm{BS}} = 80$.

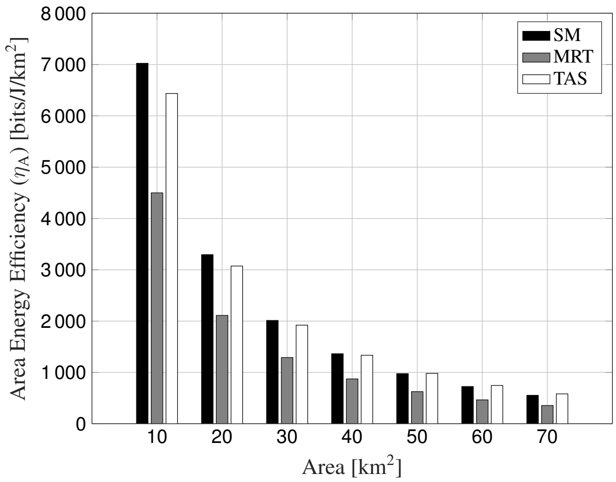

Fig. 13. Area energy efficiency (η_{A}) as a function of the coverage area with $\kappa = 1$ and $N_{\mathrm{BS}} = 80$.

turn depends on the employed interference-mitigation scheme, and on the employed PCM, if the backhaul or the fraction that scales with the number of antennas are considered or not. As future extensions, we intend to consider other approaches such as massive MIMO [29]. For instance, it has been shown in [32] that the energy efficiency of a massive MIMO system depends strongly on the number of antennas at the BSs and on the receiver architecture. The receiver architecture is important since, compared to linear receivers, successive interference cancellation receivers have higher signal processing complexity due to ordering and filter computation. Therefore, the maximization of the AEE in massive MIMO systems by deploying the optimal number of BSs given the requirements in terms of demanded network capacity, amount of interference and employed MIMO scheme may be of particular interest.

References

[1] "Cisco visual networking index: Global mobile data traffic forecast update, 2016-2021," White Paper, Cisco, Jun. 2017.

[2] "Ericsson mobility report," White Paper, Ericsson, Nov. 2017.

[3] G. Auer, V. Giannini, C. Desset, I. Godor, P. Skillermark, M. Olsson, M. A. Imran, D. Sabella, M. J. Gonzalez, O. Blume, and A. Fehske, "How much energy is needed to run a wireless network?" *IEEE Wireless Commun.*, vol. 18, no. 5, pp. 40–49, Oct 2011.

[4] L. Liu, R. Chen, S. Geirhofer, K. Sayana, Z. Shi, and Y. Zhou, "Downlink MIMO in LTE-advanced: SU-MIMO vs. MU-MIMO," *IEEE Commun. Mag.*, vol. 50, no. 2, pp. 140–147, Feb 2012.

[5] O. K. Rayel, G. Brante, J. L. Rebelatto, R. D. Souza, and M. A. Imran, "Energy efficiency-spectral efficiency trade-off of transmit antenna selection," *IEEE Trans. Commun.*, vol. 62, no. 12, pp. 4293–4303, 2014.

[6] S. Sanayei and A. Nosratinia, "Antenna selection in MIMO systems," *IEEE Commun. Mag.*, vol. 42, no. 10, pp. 68–73, Oct 2004.

[7] N. B. Mehta, S. Kashyap, and A. F. Molisch, "Antenna selection in LTE: from motivation to specification," *IEEE Commun. Mag.*, vol. 50, no. 10, pp. 144–150, Oct 2012.

[8] A. F. Molisch, "MIMO systems with antenna selection - an overview," in *Radio and Wireless Conference (RAWCON)*, Aug 2003, pp. 167–170.

[9] C. Jiang and L. J. Cimini, "Antenna Selection for Energy-Efficient MIMO Transmission," *IEEE Wireless Communications Letters*, vol. 1, no. 6, pp. 577–580, December 2012.

[10] H. Li, L. Song, and M. Debbah, "Energy Efficiency of Large-Scale Multiple Antenna Systems with Transmit Antenna Selection," *IEEE Trans. Commun.*, vol. 62, no. 2, pp. 638–647, Feb 2014.

[11] Y. Q. Hei, C. Zhang, and G. M. Shi, "Trade-off optimization between energy efficiency and spectral efficiency in large scale MIMO systems," *Energy*, vol. 145, pp. 747 – 753, 2018. [Online]. Available: http://www.sciencedirect.com/science/article/pii/S0360544217321072

[12] E. M. Okumu and M. E. Dlodlo, "Energy efficient transmit antenna selection for MIMO systems: A cross layer approach," in *2017 IEEE 7th Annual Computing and Communication Workshop and Conference (CCWC)*, Jan 2017, pp. 1–6.

[13] Z. Wang and L. Vandendorpe, "Antenna Selection for Energy Efficient MISO Systems," *IEEE Communications Letters*, vol. 21, no. 12, pp. 2758–2761, Dec 2017.

[14] R. Hernandez-Aquino, S. A. R. Zaidi, D. McLernon, and M. Ghogho, "Energy Efficiency Analysis of Two-Tier MIMO Diversity Schemes in Poisson Cellular Networks," *IEEE Transactions on Communications*, vol. 63, no. 10, pp. 3898–3911, Oct 2015.

[15] G. Auer, V. Giannini, I. Godor, P. Skillermark, M. Olsson, M. A. Imran, D. Sabella, M. J. Gonzalez, C. Desset, and O. Blume, "Cellular energy efficiency evaluation framework," in *Vehicular Technology Conference (VTC Spring)*, May 2011, pp. 1–6.

[16] F. Heliot, M. A. Imran, and R. Tafazolli, "On the energy efficiency-spectral efficiency trade-off over the MIMO Rayleigh fading channel," *IEEE Trans. Commun.*, vol. 60, no. 5, pp. 1345–1356, May 2012.

[17] F. Richter, A. J. Fehske, P. Marsch, and G. P. Fettweis, "Traffic demand and energy efficiency in heterogeneous cellular mobile radio networks," in *Vehicular Technology Conference (VTC-Spring)*, May 2010, pp. 1–6.

[18] S. Tombaz, K. W. Sung, and J. Zander, "On metrics and models for energy-efficient design of wireless access networks," *IEEE Wireless Commun. Lett.*, vol. 3, no. 6, pp. 649–652, Dec 2014.

[19] S. Tombaz, P. Monti, K. Wang, A. Vastberg, M. Forzati, and J. Zander, "Impact of backhauling power consumption on the deployment of heterogeneous mobile networks," in *GLOBECOM*, 2011, pp. 1–5.

[20] M. Boujelben, S. B. Rejeb, and S. Tabbane, "A comparative study of interference coordination schemes for wireless mobile advanced systems," in *Int. Symp. Netw., Comput. Commun.*, Jun 2014, pp. 1–5.

[21] S. Nagata, W. Xi, X. Yun, Y. Kishiyama, and L. Chen, "Interference measurement scheme for CoMP in LTE-advanced downlink," in *Vehicular Technology Conference (VTC Spring)*, June 2013, pp. 1–6.

[22] H. Sun, H. Zhang, T. Yang, and Y. Liu, "A low complexity scheme for realistic multi-cell downlink coherent joint transmission," in *2015 IEEE 26th Annual International Symposium on Personal, Indoor, and Mobile Radio Communications (PIMRC)*, Aug 2015, pp. 759–763.

[23] D. J. Love, R. W. Heath, V. K. N. Lau, D. Gesbert, B. D. Rao, and M. Andrews, "An overview of limited feedback in wireless communication systems," *IEEE Journal on Selected Areas in Communications*, vol. 26, no. 8, pp. 1341–1365, October 2008.

[24] M. Kountouris and J. G. Andrews, "Downlink SDMA with Limited Feedback in Interference-Limited Wireless Networks," *IEEE Transactions on Wireless Communications*, vol. 11, no. 8, pp. 2730–2741, August 2012.

[25] Y. S. Fahad, T. Isotalo, J. Niemelaä, and M. Valkama, "Impact of Macrocellular Network Densification on the Capacity, Energy and Cost Efficiency in Dense Urban Environment," *International Journal of Wireless and Mobile Networks*, vol. 5, no. 5, pp. 99–118, 2013.

[26] R. Krauss, G. Brante, R. D. Souza, O. Onireti, O. K. Rayel, and M. A. Imran, "On the area energy efficiency of multiple transmit antenna small base stations," in *IEEE Global Communications Conference (2017)*, Dec 2017, pp. 1–5.

[27] A. Goldsmith, *Wireless Communications*. New York, NY, USA: Cambridge University Press, 2005.

[28] A. A. A. Suhail Najm Shahab and A. R. Zainun, "Assessment of Area Energy Efficiency of LTE Macro Base Stations in Different Environments," *J. Telecommun. and Inf. Technol.*, no. 1, pp. 59–66, 2015.

[29] E. Bjornson, L. Sanguinetti, J. Hoydis, and M. Debbah, "Optimal design of energy-efficient multi-user MIMO systems: Is massive MIMO the answer?" *IEEE Trans. Wireless Commun.*, vol. 14, no. 6, pp. 3059–3075, Jun. 2015.

[30] M. H. A. Khan, J.-G. Chung, and M. H. Lee, "Downlink performance of cell edge using cooperative BS for multicell cellular network," *EURASIP J. Wirel. Commun. Netw.*, vol. 2016, no. 1, p. 56, 2016.

[31] M. R. McKay, I. B. Collings, and P. J. Smith, "Capacity and SER analysis of MIMO beamforming with MRC," in *IEEE International Conference on Communications*, vol. 3, June 2006, pp. 1326–1330.

[32] T. Liu, J. Tong, Q. Guo, J. Xi, Y. Yu, and Z. Xiao, "Energy efficiency of uplink massive MIMO systems with successive interference cancellation," *IEEE Commun. Letters*, vol. 21, no. 3, pp. 668–671, March 2017.